

## MODAL ANALYSIS OF UPLIFTING BEHAVIOR OF BUILDINGS MODELED AS UNIFORM SHEAR-BEAM

T. Ishihara<sup>1</sup>, M. Midorikawa<sup>2</sup> and T. Azuhata<sup>3</sup>

<sup>1</sup> Senior Researcher, National Institute for Land and Infrastructure Management, Tsukuba, Japan

<sup>2</sup> Professor, Graduate School of Engineering, Hokkaido University, Sapporo, Japan

<sup>3</sup> Head, National Institute for Land and Infrastructure Management, Tsukuba, Japan

Email: ishihara-t92hd@nilim.go.jp, midorim@eng.hokudai.ac.jp, azuhata-t92ta@nilim.go.jp

### ABSTRACT :

It has been pointed out that buildings during strong earthquakes have been subjected to foundation uplift. The rocking motion accompanied by uplift can reduce the damage of the structures as mentioned in some previous studies. To understand the general properties of transient uplifting behavior of multi-story buildings, studies with simpler model and mathematical expressions are useful. In this paper, dynamic behavior of buildings allowed to uplift is investigated by means of classical modal analysis. The system considered is a uniform shear-beam model on a rigid ground. The equations of motion are derived and eigenproblem is solved to investigate the modal properties during uplift. Initial velocity analysis during the first excursion of uplift is carried out to show the responses of transient rocking motion accompanied by uplift. In addition to the confirmation of significant reduction effect, it is pointed out from the results that the relatively complicated uplift responses at a glance can be recognized as natural consequences of higher modes' properties and their behaviors.

**KEYWORDS:** rocking vibration, uplift, higher mode, equivalent modal mass and direction, potential energy of self-weight, distribution of story shear coefficient

### 1. INTRODUCTION

It has been pointed out that buildings during strong earthquakes have been subjected to foundation uplift (Rutenberg et al. 1982, Hayashi et al. 1999). Some studies dealing with foundation uplift in flexible systems have already been conducted (e.g. Muto et al. 1960, Meek 1975, 1978, Psycharis 1983, Yim et al. 1985). The authors also studied experimentally and analytically from the point of view of utilizing transient uplift motion for reduction of seismic response (e.g. Midorikawa et al. 2003, Ishihara et al. 2006a, 2006b, 2007).

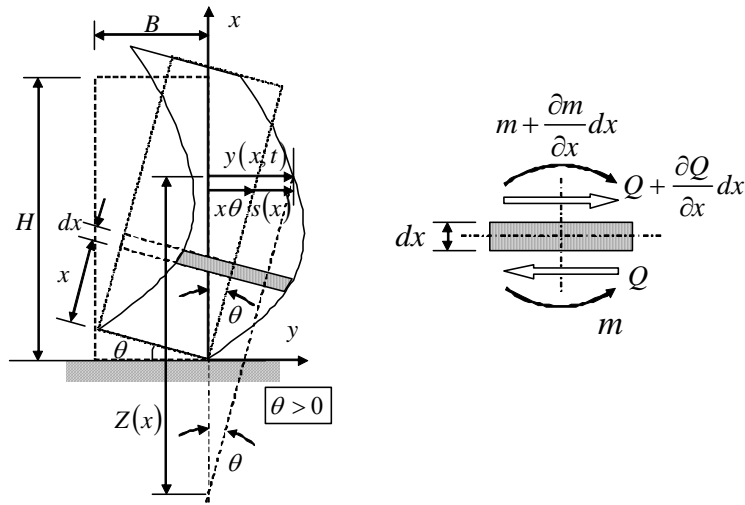
To understand the general properties of transient uplifting behavior of multi-story buildings, studies with simpler model and mathematical expressions are useful.

In this paper, dynamic behavior of buildings allowed to uplift is investigated by means of classical modal analysis. The system considered is a uniform shear-beam model on a rigid ground. It represents multi-story buildings allowed to rock accompanied with uplift motion without sinking into the ground.

### 2. SYSTEM CONSIDERED AND MODAL PROPERTIES

#### 2.1. System considered

Figure 1(a) shows a uniform shear-beam model allowed to uplift with a typical segment of infinitesimal height  $dx$  located at the distance  $x$  from the base. The base of the system is constrained against horizontal motion, so no deformation and slippage is allowed between the base and the ground. It is assumed that the section is rigid and that displacement is small enough not to need to consider the so-called  $P-\Delta$  effect. Generally speaking, an ordinary multi-story building does not have the constant story shear stiffness through the height. In slender buildings, deformations due to columns' shortening/elongation should be often considered. Nevertheless we adopt the uniform shear-beam model to make the mathematical expressions of motions as simple as possible and to reduce the number of structural parameters.



(a) Uniform shear-beam model allowed to uplift (b) Free body diagram of a typical segment  
Figure 1 System considered

## 2.2. Eigenproblem

Equations of motion of the segment (see Fig. 1(b)) for free vibration during uplift are as follows :

$$\text{Horizontal : } \rho A dx \cdot \ddot{y} = Q' dx \quad (2.1)$$

$$\text{Rotational : } \rho A dx \left( \frac{B^2}{3} \right) \ddot{\theta} = m' dx + Q dx \quad (2.2)$$

where  $\rho A$  is the mass per unit height,  $y = y(x, t) = x\theta + s(x)$  is horizontal displacement,  $s = s(x, t)$  is horizontal displacement due to shear deformation,  $\theta(t)$  is rotational angle of the section,  $Q = rs'$  is shear force,  $r$  is shear stiffness,  $B$  is width or span,  $m$  is bending moment. The dots and primes signify differentiation with respect to time  $t$  and coordinate  $x$ .

Provided that the displacement is small, we can recognize the motion of the segment to be the rotation with radius  $Z(x)$ . So we can write the displacement  $y(x, t) = Z(x)\theta(t)$ . Let us denote the circular frequency by  $p$ . For free vibration,  $\ddot{\theta} = -p^2\theta$ . Considering the boundary condition, the mode shape (eigenvector)  $Z(x)$  is defined as

$$Z(x)/H = (Z_H/H) \left\{ \frac{\sin(\xi x/H)}{\sin \xi} \right\}, \quad Z_H/H = \tan \xi / \xi \quad (2.3a,b)$$

where  $\xi = pH\sqrt{\rho A/r}$  is dimensionless frequency and  $H$  is the height. The subscript “ $H$ ” denotes the location at the top, i.e.  $x = H$ . Note that Eqn.2.3 defines the length of the eigenvectors, not within a scalar multiple. If  $\xi$  approaches zero, the mode shape converges that of rigid block, i.e.  $Z(x) \rightarrow x$ , when  $\xi \rightarrow 0$ . Integrating Eqn. 2.2 over the height, we obtain the frequency equation for the case under consideration.

$$1 - Z_H/H = \left\{ \frac{B^2}{(3H^2)} \right\} \xi^2 \quad (2.4)$$

Because Eqn. 2.4 is transcendental, the dimensionless frequencies must be found numerically. The roots of Eqn. 2.4 may be envisioned as representing the intersection of the function of  $\xi$  on the left-hand side and the quadratic function of  $\xi$  and  $H/B$  on the right-hand side. Figure 2 shows an example of functions on both sides of Eqn. 2.4. The values of  $\xi$  at the intersections are the dimensionless frequencies in an uplifting phase. The first mode has zero frequency corresponding to the rigid body mode rotating around the edge of the base.

Vertical dashed lines show the dimensionless frequencies  $\xi_{ff}$  in full contact with the ground, where  $\xi_{ff} = p_{ff} H \sqrt{\rho A / r} = (2j-1)\pi/2$  ( $j=1,2,\dots$ ), in which  $p_{ff}$  is the corresponding circular frequency of mode  $j$ . Eigenvalue separation property (e.g. Bathe 1996), which is well known as a general property of eigenvalue problems, can be seen in the figure, i.e.  $\xi_j < \xi_{ff} < \xi_{j+1}$ .

Figure 3 shows the relationships between  $\xi_j$  and  $H/B$ . For relatively slender structures, the second frequency is nearly equal to or slightly less than that in full contact phase. The more slender the structure is, the larger the higher frequencies become.

Figure 4 shows the mode shapes for an uplifting phase rocking around the right edge of the base.

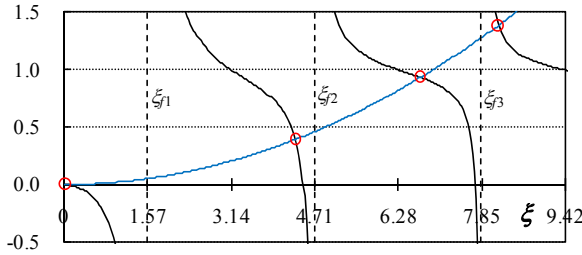
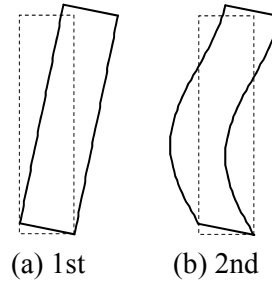


Figure 2 Functions of  $\xi$  in Eqn. 2.4 ( $H/B=4$ )



(a) 1st

(b) 2nd

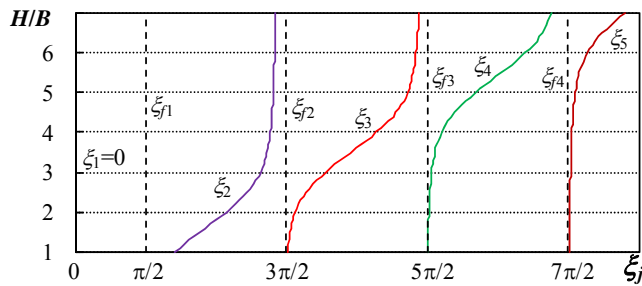
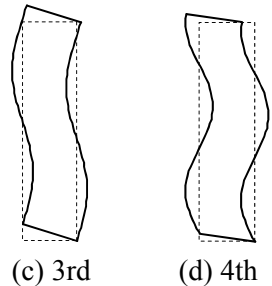


Figure 3 Dimensionless frequency



(c) 3rd

(d) 4th

Figure 4 Mode shape ( $H/B=4, \theta_j > 0$ )

Let us confirm the orthogonal properties by considering modes  $j$  and  $k$ . For  $j \neq k$ , orthogonality relationships can be derived as ,

$$\rho A \int Z_j Z_k dx + MB^2/3 = 0, \quad r \int (Z'_j - 1)(Z'_k - 1) dx = 0 \quad (2.5a,b)$$

For  $j=k$ ,

$$\rho A \int Z_k^2 dx + MB^2/3 \equiv I_k, \quad r \int (Z'_k - 1)^2 dx = -p_k^2 I_k \quad (2.6a,b)$$

where  $I_k$  is the moment of inertia of mode  $k$  with respect to  $\theta_k$ ,  $M = \rho A H$  is the total mass of the structure. Note that the magnitude of  $I_k$  is fixed because the eigenvectors  $Z(x)$  is defined not within a scalar multiple in Eqn.

2.3.  $I_k$  can be calculated as a function of  $\xi_k$ ,  $I_k = MH^2 \left[ \left\{ 1 - (\sin 2\xi_k) / 2\xi_k \right\} / \left\{ 2\xi_k^2 \cos^2 \xi_k \right\} + B^2 / (3H^2) \right]$

(when  $\xi_k \rightarrow 0$ , the value of  $I_k$  approaches that of rigid block, i.e.  $I_k \rightarrow MH^2/3 + MB^2/3$ ).

### 2.3. Equivalent modal mass and direction

Now let's consider the equivalent single degree of freedom (SDOF) system for each mode. In an uplifting phase, each mode must have the equivalent modal mass and direction because two dimensional motions are caused, while the equivalent direction in full contact phase is just horizontal. To define the equivalent mass and direction, momentum and energy of the equivalent SDOF system should be set to be equal to those of each mode with respect to  $\theta_k$ .

$$S_{hk} = M_k H_k, \quad S_v = M_k B_k, \quad I_k = M_k (H_k^2 + B_k^2) \quad (2.7a,b,c)$$

where  $S_{hk} \equiv \rho A \int Z_k dx = MH(1 - \cos \xi_k) / (\xi_k^2 \cos \xi_k)$  (when  $\xi_k \rightarrow 0$ ,  $S_{hk} \rightarrow MH/2$ ),  $S_v \equiv MB/2$ ,  $M_k$  is the equivalent (or effective) mass for mode  $k$ ,  $H_k$  and  $B_k$  are the height and width of the equivalent SDOF system respectively as illustrated in figure 5(a). The symbol  $\phi_k$  represents the direction of mode  $k$ ,  $\phi_k = \tan^{-1}(S_v/S_{hk})$ . Note that the sum of  $M_k$  is equal to  $7M/4$  because the sum of vertical total mass decomposed into the modal equations is  $3M/4$  due to the assumption that the section is rigid. The relationships between  $M_k$  and the ordinary equivalent modal masses for horizontal  $M_{hk}$  and vertical  $M_{vk}$  of mode  $k$  are,

$$M_{hk} = M_k \cos^2 \phi_k, \quad M_{vk} = M_k \sin^2 \phi_k \quad (2.8a,b)$$

Figure 6 is a vector type representation of the equivalent mass – spring systems illustrated in figure 5(b). The length and the direction of the vector represent the ratio of the equivalent mass  $M_k/M$  and direction  $\phi_k$ . In this figure, we set  $0 < \phi_k < \pi$ . If the structure rocks around the left edge of the base (i.e.  $\theta < 0$ ), the figure changes into the symmetric one with respect to the y-axis of the graph. The first, rigid mode has the mass of  $3M/4$ , and its direction is perpendicular to the line connecting the right edge of the base and the center of the mass. The third mode has the direction about  $\pi/2$ . For an uplift phase even if the ground motions stop, the modes having relatively large equivalent mass and the direction about  $\pm\pi/2$  can be well oscillated around the static equilibrium state because the gravity acts vertically and suddenly just after the lift-off as a step function. But the contributions of those modes to base shear response are little as shown later.

Figure 7 shows the relationships between the structural parameter  $H/B$  and the equivalent modal properties. For slender structures, the third and higher modes still have the equivalent mass of about  $0.5M$  at the maximum. The absolute value of directional angles of the first and the second modes are nearly equal to or less than 45 degrees, while those of the third and higher modes reaches about 90 degrees at the maximum.

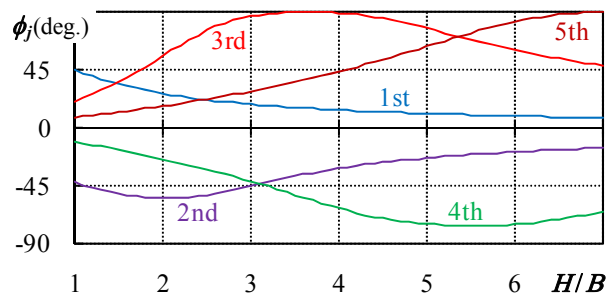
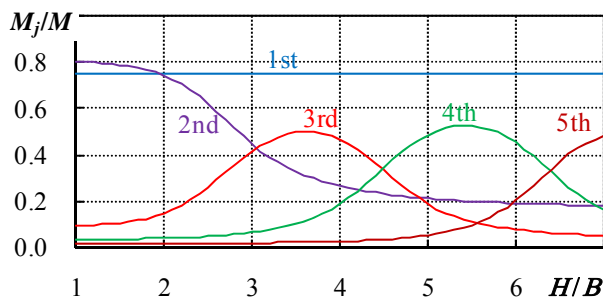
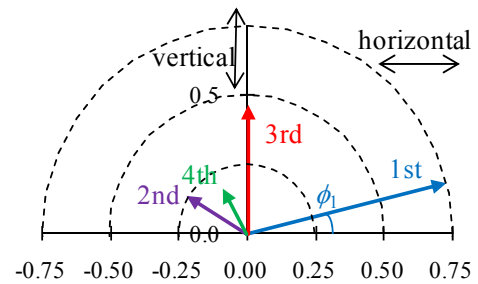
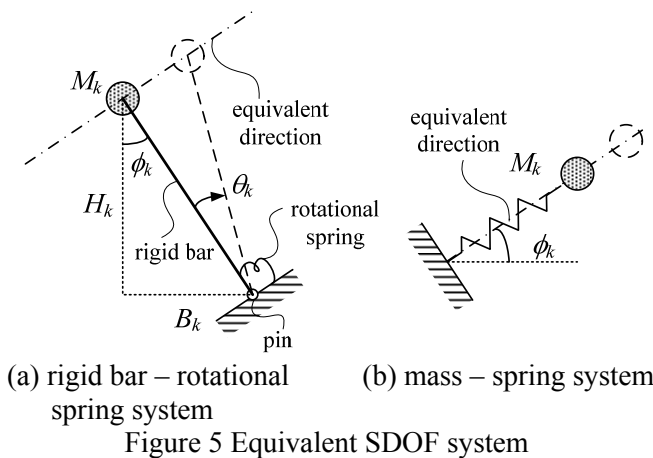


Figure 7 Equivalent modal mass and direction

### 3. INITIAL VELOCITY ANALYSIS

To grasp the general properties of dynamic behavior of rocking motion accompanied by uplift, initial velocity analysis is carried out utilizing the modal equations. Suppose that the system initially at rest on the ground is subjected to the impulsive horizontal forces having the same distribution shape along the height as that of the first mode in full contact phase (i.e. fixed base condition). The system begins to vibrate only in the first mode. If the system oscillates enough, the base of the structure begins to rock accompanied by uplift motion when the overturning moment reaches the resisting moment due to gravity,  $MgB/2$ . The analysis is conducted between the instant of time of initiation of uplift and that of landing, that is, the first excursion or half cycle of uplifting behavior. As a basic study, ground motions and damping of the system are neglected.

#### 3.1. Equations of motion

We can express the horizontal displacement  $y(x, t)$  and rotation  $\theta(t)$  by superimposing the modal responses, i.e.  $y(x, t) = \sum Z_j(x)\theta_j(t)$  and  $\theta(t) = \sum \theta_j(t)$ . Substituting these equation into Eqn.2.1 and 2.2, adding the effect of gravity  $-\text{sgn}(\theta)\rho A dxgB/2$  to the right-hand side of Eqn. 2.2, integrating the both Eqns. over the height after multiplying Eqn. 2.1 by  $Z_k(x)$ , adding the results together, the equation of motion for mode  $k$  can be derived as,

$$I_k \ddot{\theta}_k + p_k^2 I_k \theta_k = -\text{sgn}(\theta) S_v g \quad (3.1)$$

where  $g$  is gravitational acceleration. Let us introduce dimensionless time  $\tau = p_{f1}t$ , rigid component of horizontal displacement at the top  $\delta_k = H\theta_k$  and dimensionless pseudo acceleration (Meek, 1978)  $a_k = p_{f1}^2 \delta_k / g$ . Eqn. 3.1 can be changed to,

$$\frac{d^2 a_k}{d\tau^2} + \left( \frac{\xi_k}{\xi_{f1}} \right)^2 a_k = -\text{sgn}(\theta) \frac{S_v H}{I_k} \quad (3.2)$$

The analytical solutions of Eqn. 3.2 can be found easily.

For the representation of the results in the next section, we assume  $t = \tau = 0$  at the instant of initiation of uplift and  $\theta > 0$  after lift-off. Initial conditions of modes for an uplift phase can be derived using the orthogonal properties of modes with  $\theta(0) = 0$  and  $(d\theta/d\tau)_{\tau=0} = 0$ . Up to 10 modes are used to calculate the responses.

#### 3.2. Time histories and modal contributions

Figure 8 shows an example of time histories of responses during the first uplifting excursion with the modal contributions. Note that the input level of impulsive forces is appropriately measured by the base shear coefficient under fixed base condition,  $C_{Bf}$ . In the case of the figure, we assume  $C_{Bf} = 0.6$  and  $H/B = 4$ . Horizontal displacement at the top and rotation due to uplift ( $a = \sum a_j$ ) are represented as dimensionless pseudo accelerations. It should be noted that the rotations in the second and the higher modes are minus almost all the time during uplift, whereas that of the first, rigid body mode is plus. So we can recognize an uplift behavior as the sum of largely uplifting response of the first mode and vibrations of higher modes accompanied with slight sinking. From the point of view of utilizing transient uplift motion for reduction of seismic response to absorb the vibration energy as potential energy of self weight, the first mode is effective, but higher modes have to absorb a part of potential energy of self weight as their strain energy. This is the main reason why the effect of higher modes is well observed during uplift (e.g. Ishihara et al. 2007). From the figure 8(a) and (b), horizontal displacement and rotation due to uplift are dominated mainly by the first, rigid body mode. On the other hand, base shear coefficient  $C_B$ , overturning moment coefficient  $C_m$  and strain energy  $We$  are affected by higher modes while the first mode has no effect on these responses because of the rigid body mode. Note that the overturning moment coefficient  $C_m$  is defined as  $m_{ovt}/(MgH/2)$ , where  $m_{ovt}$  is

overturning moment calculated by integrating the moment  $Qdx$  of the segment over the height. The phenomena are due to the modal properties for an uplifting phase as described in the preceding chapter. For example, the third mode's contribution to the base shear is little because of its modal direction. Figure 8(f) shows the potential energy of self weight  $Wp$  as a fraction of total energy  $E_{all}$ . In this case, 87% of total energy was stored temporarily as the potential energy of self weight, while the maximum strain energy is only 29%. Figure 9 shows an example of the dynamic load – displacement relationships under the same condition in figure 8. Higher modes' behaviors during uplift make the curves relatively complicated.

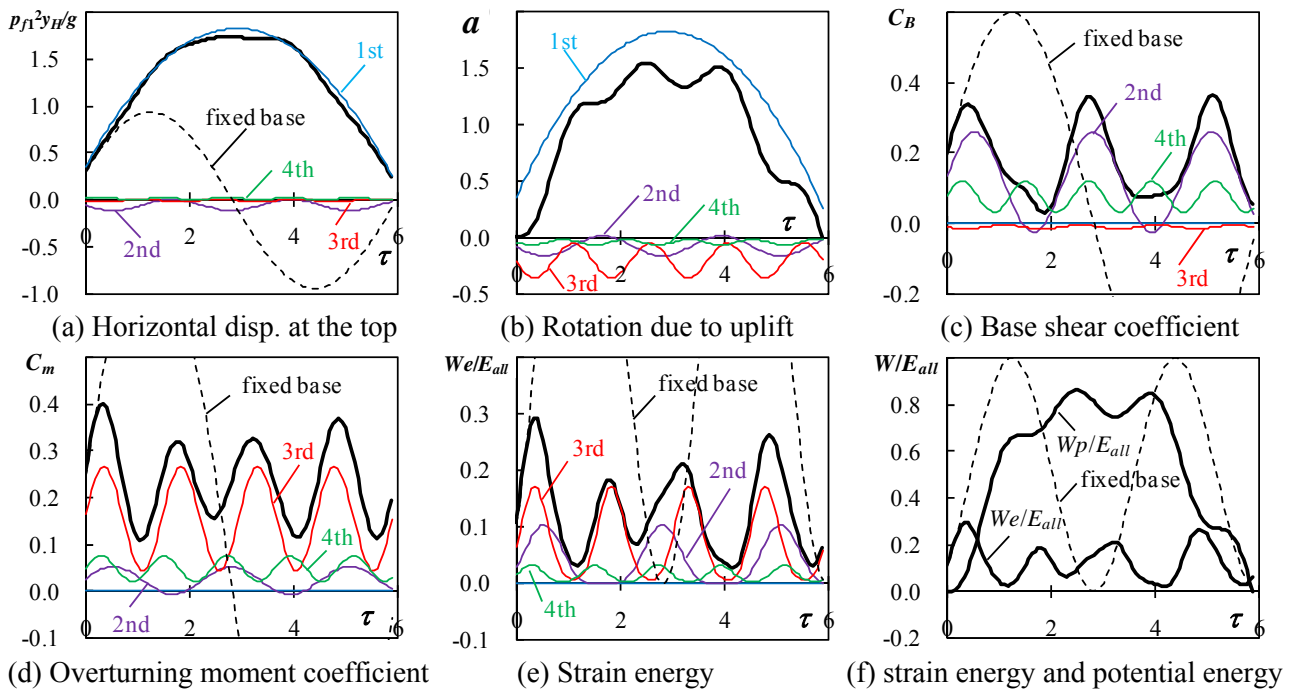


Figure 8 Time histories and modal contribution ( $H/B=4$ ,  $C_{Bf}=0.6$ )

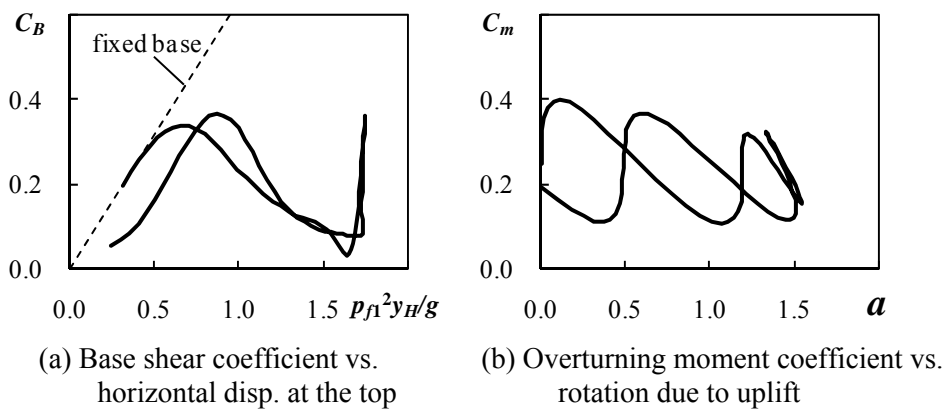


Figure 9 Dynamic load – displacement relationship ( $H/B=4$ ,  $C_{Bf}=0.6$ )

### 3.3. Reduction effect due to uplift

Figure 10 summarizes the maximum responses to show the reduction effect owing to uplift. Thick and thin lines show the maximum and minimum responses respectively. The figure also shows the range of input level where the overturning moment always remains plus during the incipient uplift excursion, that is, the right edge keeps on touching with the ground. The two degrees of freedom version corresponding to figure 10(a) can be found in the literature (Meek, 1975). By allowing uplift, the maximum base shear, overturning moment and strain energy are significantly reduced, especially in slender structures. For example, under the input level

of  $C_{Bf} = 0.8$ , the maximum base shears of the structures of  $H/B=3, 4$  and  $6$  are reduced to  $0.55, 0.44$  and  $0.40$  of the total weight respectively. The maximum strain energy as a fraction of total energy is less than 30% under the condition of  $H/B \geq 4$  and  $C_{Bf} \geq 0.6$ .

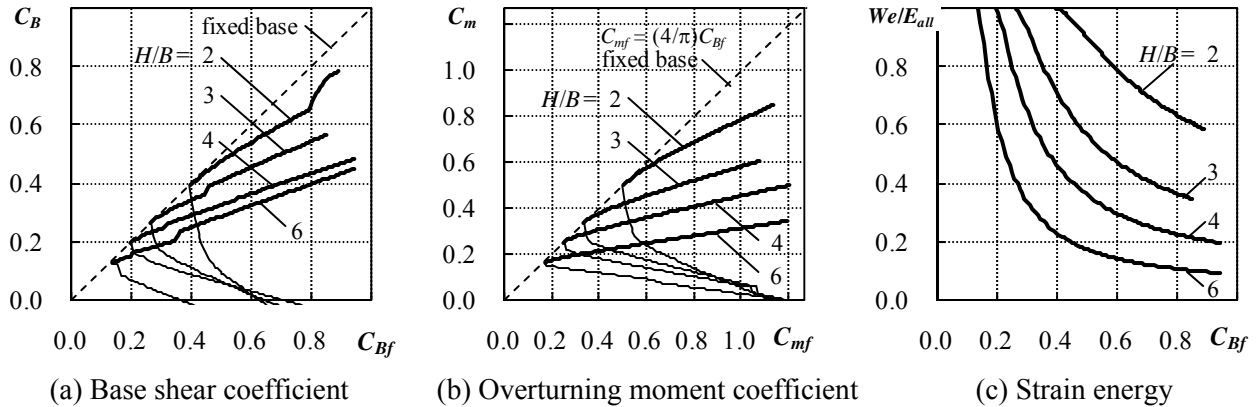


Figure 10 Reduction effect due to uplift

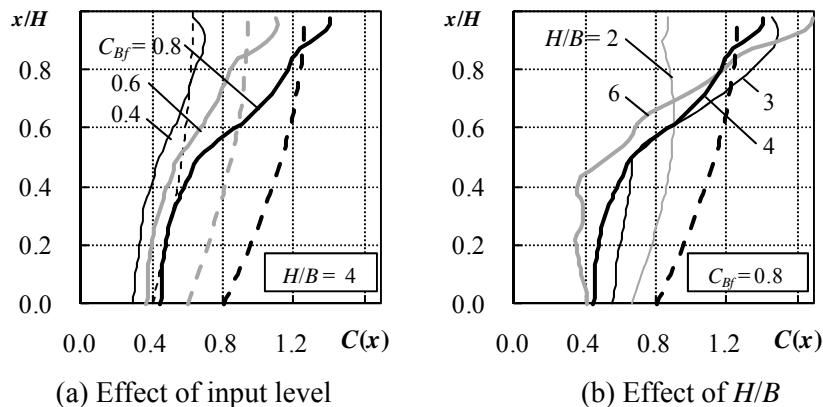


Figure 11 Story shear coefficient

Figure 11 shows the maximum story shear coefficient  $C(x)$  along the height. Dashed lines show those of fixed base structures vibrating only in its first mode. Story shears including the base shear are increased with the input level, particularly in the upper part. For slender structures, story shear is reduced in the lower part of the structure, but increased in the upper part. Allowing uplift changes the distribution of story shear force coefficient along the height into somewhat top heavy one. Similar tendency was also found in the results of analytical and experimental studies of discrete mass systems (Ishihara et al., 2006a, 2007). This tendency can be recognized as the natural consequence of the properties and behaviors of higher modes during uplift.

#### 4. CONCLUSIONS

In this paper, uniform shear-beam model is used as a representation of multi-story buildings allowed to uplift. The modal properties and dynamic behaviors during an uplift excursion are clarified by defining the equivalent single degree of freedom system of each mode and conducting the initial velocity analysis as the sum of modal responses to be able to calculate analytically. From the results, the conclusions are summarized as follows:

- (1) For slender structures, higher modes during uplift can still have relatively large equivalent modal masses of about half of the total mass at the maximum, and their modal directions can be close to vertical. These properties of higher modes cause relatively complicated responses during uplift.
- (2) Transient uplifting behavior can be decomposed into largely uplifting response of the first, rigid body mode and vibrations of higher modes accompanied with slight sinking.

- (3) Higher modes have to absorb a part of potential energy of self weight as their strain energy. This is the main reason why higher mode effect is well observed during uplift.
- (4) Top and uplift displacements are dominated mainly by the first, rigid body mode. On the other hand, stresses in the structure are caused by higher modes.
- (5) Higher modes during transient uplift motion change the shape of distribution of shear forces along the height into somewhat top heavy one.

## ACKNOWLEDGEMENT

Part of this work is supported by the Ministry of Education, Culture, Sports, Science and Technology (MEXT) of Japan under Grant-in-Aid for Scientific Research, Project No. 19560590 and 19360244.

## REFERENCES

- Bathe, K. J. (1996). Finite element procedures, Prentice-Hall
- Hayashi, Y., Tamura, K., Mori, M. and Takahashi, I. (1999). Simulation analyses of buildings damaged in the 1995 Kobe, Japan, earthquake considering soil-structure interaction. *Earthquake Engineering and Structural Dynamics* **28:4**, 371-391.
- Ishihara, T., Midorikawa, M. and Azuhata, T.(2006a). Vibration characteristics and dynamic behavior of multiple story buildings allowed to uplift, *Proceedings of SPIE*, **6169**, 61691A-1-8
- Ishihara, T., Azuhata, T. and Midorikawa, M.(2006b). Effect of dampers on dynamic behavior of structures allowed to uplift, *STESSA2006*, 709-715
- Ishihara, T., Azuhata, T., Noguchi, K., Morita K. and Midorikawa, M.(2007). Shaking table test on seismic response of reduced scale models of multi-story buildings allowed to uplift, *Earthquake Resistant Engineering Structures* **6**, 175-184
- Meek, J.W. (1975). Effects of foundation tipping on dynamic response, *Journal of the Structural Division*, **101:ST7**, 1297-1311
- Meek, J.W. (1978). Dynamic response of tipping core buildings, *Earthquake Engineering and Structural Dynamics* **6**, 437-454.
- Midorikawa, M., Azuhata, T., Ishihara, T., and Wada, A. (2006). Shaking table tests on seismic response of steel braced frames with column uplift. *Earthquake Engineering and Structural Dynamics* **35:14**, 1767-1785.
- Muto, K., Umemura, H. and Sonobe, Y.(1960). Study of the overturning vibrations of slender structures, *Proceedings of the Second World Conference on Earthquake Engineering*, Tokyo
- Psycharis, I. N.(1983). Dynamics of flexible systems with partial lift-off, *Earthquake Engineering and Structural Dynamics*, **11**, 501-521
- Rutenberg, A., Jennings, P. C. and Housner, G. W. (1982). The response of veterans hospital building 41 in the San Fernando earthquake. *Earthquake Engineering and Structural Dynamics* **10:3**, 359-379.
- Yim, C. S. and Chopra, A. K. (1985). Simplified earthquake analysis of multistory structures with foundation uplift, *Journal of Structural Engineering*, **111:12**, 2708-2731

## APPENDIX

The typical values of dimensionless frequencies  $\xi_j$  are listed in table A.1.

Table A.1 Dimensionless frequencies

H/B	$\xi_1$	$\xi_2$	$\xi_3$	$\xi_4$	$\xi_5$
1	0	2.204	4.745	7.860	10.998
2	0	3.352	4.911	7.884	11.006
3	0	4.131	5.578	7.948	11.021
4	0	4.350	6.697	8.160	11.054
5	0	4.415	7.392	8.923	11.132
6	0	4.444	7.579	10.029	11.402
7	0	4.459	7.640	10.613	12.273